


Immune Stimulating Outcome of Chrysin and γ -Irradiation via Apoptotic Activation Against Solid Ehrlich Carcinoma Bearing Mice

Integrative Cancer Therapies
Volume 21: 1–12
© The Author(s) 2022
Article reuse guidelines:
sagepub.com/journals-permissions
DOI: 10.1177/15347354221096668
journals.sagepub.com/home/ict


Nermeen M. El Bakary, PhD¹ , Asmaa Z. Alsharkawy, PhD²,
Zeinab A. Shouaib, PhD², and Emad M.S. Barakat, PhD³

Abstract

The rising interest in innovative methods of cancer immunotherapy has prompted research into the immunomodulatory mechanisms of natural and synthetic substances. The goal of this study was to assess chrysin immune-stimulating and pro-apoptotic effects on tumor growth and cell susceptibility to ionizing radiation in order to improve cancer therapy. Chrysin (20 mg/kg/day) was intraperitoneally injected to mice bearing 1 cm³ solid tumor of Ehrlich ascites carcinoma (EAC) for 21 consecutive days. Mice were whole body exposed to 1 Gy of gamma radiation (2 fractionated dose 0.5 Gy each). Treatment with chrysin dramatically reduces tumor proliferation in EAC mice; furthermore, IFN- γ activity is significantly reduced when compared to EAC mice. When compared to EAC mice, the expression of TNF- α , free radicals, and nitric oxide (NO) levels were considerably reduced, along with improvements in apoptotic regulators (caspase-3 activity). Moreover, the histopathological investigation confirms the improvement exerted by chrysin even in the EAC mice group or the EAC + R group. What is more, exposure to gamma radiation sustained the modulatory effect of chrysin on tumor when compared with EAC + Ch mice. Hence, chrysin might represent a potential therapeutic strategy for increasing the radiation response of solid tumor.

Keywords

chrysin, gamma radiation, TNF- α , IFN γ , apoptosis, caspase-3, histopathology

Submitted November 26, 2021; revised March 12, 2022; accepted April 8, 2022

Introduction

Cancer is one of the most common causes of morbidity and mortality around the world. Despite the fact that deaths from communicable diseases have decreased as a result of medical advancements, cancer-related deaths have increased by 40% in recent years. The number of cancer patients is expected to rise in the future, with up to 13 million cancer-related fatalities expected by 2030. There are several issues with providing effective cancer therapy, including the inadequacy of currently used medicines, a lack of early detection, and a lack of understanding of the signaling networks involved in cancer malignancy.¹ Hence, discovering an approach to treat cancer at numerous stages could assist in rescuing people's lives. Notably, cancers can be treated by combinations of surgical procedures, radiation therapy, chemotherapy, immunotherapy, and hormone therapy. Meanwhile, chemotherapy is one of the most reasonable

cures for early- and late-stages; nevertheless, alopecia, neuropathy, neutropenia, myalgia, nausea, vomiting, diarrhea, and fatigue are the side effects of chemotherapy that lead to less compliance of patients.²

The rising interest in innovative methods of cancer immunotherapy, as well as a high demand for therapeutic medicines that can control various forms of immunodeficiency, has prompted research into the immunomodulatory

¹National Centre for Radiation Research and Technology, Egyptian Atomic Energy Authority, Cairo, Egypt

²Al-Azhar University, Cairo, Egypt

³Ain Shams University, Cairo, Egypt

Corresponding Author:

Nermeen M. El Bakary, Radiation Biology Department, National Centre for Radiation Research and Technology, Egyptian Atomic Energy Authority, Nasty-Cairo, Cairo 11765, Egypt.
Email: nermeen_ahmed11@yahoo.com



mechanisms of natural and synthetic substances. The resinous substance collected by honey bees from various plant sources and used by bees to plug gaps in their honeycombs, smooth down the inside walls, and secure the entrance against intruders is known as propolis (bee glue). It contains a diverse range of biological elements, including polyphenols, flavonoids, glycones, phenolic acid and its esters, phenolic aldehydes and ketones, terpenes, sterols, vitamins, amino acids, etc.³ In our recent work, we have shown that propolis has a pronounced cytostatic, anti-carcinogenic, and antitumor effect both in *in vitro* and *in vivo* tumor models.⁴ It has been suggested that the therapeutic activities of propolis depend mainly on the presence of flavonoids. Flavonoids have also been reported to induce the immune system, and to act as strong oxygen radical scavengers.⁵

Chrysin (5,7-dihydroxyflavone), a flavonoid found in honey, propolis, and many plant species, belongs to the flavonoid family. Flavonoids have a wide range of biological actions, including antitumor, immunomodulatory, anti-inflammatory, anti-allergy, antioxidant, and cardioprotective properties. Chrysin is one of a vast group of polyphenolic compounds found in food and numerous herbal items that have long been linked to a number of key biochemical and pharmacological activities in cancer prevention and health promotion.¹

Low dose gamma irradiation has been authenticated as a promising auxiliary strategy to improve the immune adaptive response and its implication during the strategy of cancer treatment indicates many intriguing results. Feinendegen reported that radiation hormesis is the hypothesis for why low doses of ionizing radiation (IR) are beneficial, stimulating the activation of repair mechanisms that protect against disease, which are not activated in absence of IR. A low dose of IR is a dose that creates a burst of hits and ROS that is adequate to stimulate the protective systems and produce observable health benefits, within the region of and just above natural background levels in the range 0.01 to 0.50 Gy. Hence, the radiation adaptive response directs DNA repair and gives the impression of being a central origin of the prospective hormetic effect.⁶⁻⁸

This led us to compare how the administration of polyphenolic compound deriving from propolis influences Ehrlich ascites tumor growth. The present work was an endeavor to evaluate the immune stimulating and proapoptotic effect of chrysin on tumor growth and cell sensitivity to IR, targeting the improvement of cancer therapeutic protocols.

Materials and Methods

Animals

Adult female Swiss albino mice weighing 25 to 30 g were supplied from the animal breeding house of the National

Center for Radiation Research and Technology (NCRRT). Mice were acclimatized in the animal facility of NCRRT for at least 1 week under temperature and humidity controlled rooms ($25^{\circ}\text{C} \pm 2^{\circ}\text{C}$ and $60\% \pm 5\%$, respectively) before subjecting them to experimentation. Animals were fed a commercial standard pellet diet and water *ad libitum* during this period.

Ethics Statement

This study was conducted in accordance with the recommendations in the Guide for the Use and Care of Laboratory Animals of the National Institute of Health (NIH no. 85:23, revised 1996) and in compliance with the regulations of Ethical Committee (REC) of the National Center for Radiation Research and Technology (NCRRT), Atomic Energy Authority, Cairo, Egypt (Approval Number: 28A/21). REC has approved this research protocol, following the 3Rs principles for animal experimentation (Replace, Reduce, and Refine) and is organized and operated according to the CIOMS and ICLAS International Guiding Principles for Biomedical Research Involving Animals 2012.

Drugs and Chemicals

Chrysin and other chemicals and reagent in this study were obtained from Sigma-Aldrich Chemical Co. (Gillingham, UK). Chrysin was dissolved in DMSO and injected *i.p.* at a dose of 20 mg/kg body weight according to Villar *et al.*,⁹ for 21 consecutive days.

Radiation Facility and Irradiation Procedures

Mice were exposed to whole body γ -irradiation at a cumulative dose of 1 Gy divided into 2 fractions; 0.5 Gy/each fraction, which was performed at NCRRT using the Gamma cell 40 (Cs^{137}) biological irradiator manufactured by the Atomic Energy of Canada Limited, Ottawa, Ontario, Canada. Animals were placed in a plastic sample tray with lid and supports provided for use in the sample cavity. The unit has ventilation holes which align with ventilation parts through the main shield to provide a means for uniform irradiation for small animals at a dose rate of 0.403 Gy/minute at the time of experiment according to the guidelines of the Protection and Dosimetry Department.

Tumor transplantation

In the present study the cell line of Ehrlich Ascites Carcinoma (EAC) was used as a model of solid carcinoma by inoculation in the right thigh of albino mice. The parent line was supplied as gift from the Egyptian National Cancer Institute (NCI), Cairo University. Human breast cancer is

the source of EAC cells modified to grow in female Swiss albino mice. The cell line of EAC was maintained by intraperitoneal injection (i.p.) of 2.5 million cells per animal. Bright line hemocytometer was used to count the EAC before i.p. injection and the dilution was done using physiological sterile saline solution. In order to develop Ehrlich solid tumor (EST) in the thigh, 0.2 ml EAC cells (2.5×10^6 cells /mouse) were inoculated subcutaneously (s.c.) in the right thigh of the lower limb of female mouse.¹⁰

Experimental Design

In this study, we used 75 mice weighing about 25 to 30 g. All the experiments were conducted under National Research Centre guidelines for the use and care for laboratory animals and were approved by an independent ethics committee of the NCRRT. The mice were assigned randomly to 5 equal groups of 15 mice each as follows:

Group (1): Control (C): Mice neither treated nor irradiated.

Group (2): (EAC): Mice bearing solid Ehrlich tumor.

Group (3): (EAC + R): Mice bearing solid Ehrlich tumor were subjected to 1 Gy whole body γ -irradiation (2 fractionated dose) first at 11 days post EAC inoculation and second at the day 14 post EAC formations.

Group (4): (EAC + Ch): Mice bearing solid Ehrlich tumor were injected i.p. with chrysin for 21 consecutive days starting at the day 11 after EAC inoculation (after the tumor has reached 1 cm³).

Group (5): (EAC + Ch + R): Mice bearing solid Ehrlich tumor were injected with chrysin as in group 4 along with a first whole body γ -irradiation at a dose level of 0.5 Gy 30 minutes after the first injection of Ch and the second dose of irradiation as in group 3.

Tumor Volume Monitoring

Tumor volume was measured at different time intervals during the experimental period using a Vernier caliper on the 7th, 15th, 21th days from time the tumor reached 1 cm³ during the experimental period. The volume of solid tumor was calculated using formula $[A \times B^2 \times 0.52]$, where A and B are the longest and the shortest diameter of tumor, respectively.¹¹

Tissue Collection and Preparation of Crude Tissue Homogenates

At the end of the experiment (after 24 hours), mice were anesthetized with gentle diethyl ether. Blood was collected in test tubes, and then centrifuged at 4000 g (4°C for

15 minutes) using a centrifuge (Hettich Universal 32A, Germany), and the obtained sera were stored at -20° for further analysis. The skeletal muscle (normal control), tumor tissues, and liver tissues were dissected out, and then washed with normal saline and weighed. Thereafter, they were homogenized in phosphate buffer (0.1 M, pH 7.4, ice cold) at a ratio of 1:10 times (w/v), using a Teflon Homogenizer (Universal laboratory aid, Type MPW-309, Poland), and were collected for biochemical investigations.

Biochemical Assays

Quantitative real-time PCR. RNA isolation and reverse transcription: RNA was extracted from the tumor tissue homogenate using the RNeasy plus mini kit (Qiagen, Venlo, The Netherlands), according to the manufacturer's instructions. Genomic DNA was eliminated by a DNase-on-column treatment supplied with the kit. The RNA concentration was determined spectrophotometrically at 260 nm using the Nano Drop ND-1000 spectrophotometer (Thermo Fisher scientific, Waltham, USA) and RNA purity was checked by means of the absorbance ratio at 260/280 nm. RNA integrity was assessed by electrophoresis on 2% agarose gels. RNA (1 μ g) was used in the subsequent cDNA synthesis reaction, which was performed using the Reverse Transcription System (Promega, Leiden, The Netherlands). Total RNA was incubated at 70°C for 10 minutes to prevent secondary structures. The RNA was supplemented with MgCl₂ (25 mM), RTase buffer (10X), dNTP mixture (10 mM), oligo (t) primers, RNase inhibitor (20 U), and AMV reverse transcriptase (20 U/ μ l). This mixture was incubated at 42°C for 1 hour.

Quantitative real time PCR: qRT-PCR was performed in an optical 96-well plate with an ABI PRISM 7500 fast sequence detection system (Applied Biosystems, Carlsbad, California) and universal cycling conditions of 40 cycles of 15 seconds at 95°C and 60 seconds at 60°C after an initial denaturation step at 95°C for 10 minutes. Each 10 μ l reaction contained 5 μ l SYBR Green Master Mix (Applied Biosystems), 0.3 μ l gene-specific forward and reverse primers (10 μ M), 2.5 μ l cDNA, and 1.9 μ l nuclease-free water. The sequences of PCR primer pairs used for each gene are shown in Table 1. Data were analyzed with the ABI Prism sequence detection system software and quantified using the v1.7 Sequence Detection Software from PE Biosystems (Foster City, CA). Relative expression of studied genes was calculated using the comparative threshold cycle method. All values were normalized to the endogenous control GAPDH.¹²

ELISA detection. Enzyme-linked immune sorbent assays (ELISA) for levels of IFN- γ and caspase-3 were performed using ELISA Kit (R& D Systems) according to the

Table 1. Primers used for QRT-PCR.

Primer	Sequence
TNF- α	Forward: 5'-ACGGCATGG ATCTCAAAGAC-3' Reverse: 5'-CGGACTCCGCAAAGTCTAAG -3'
GAPDH	Forward: 5'-CTCCATTCTTCCACCTTTG-3' Reverse: 5'-CTTGCTCTCAGTATCCTTGC-3'

manufacturer's instructions on the supernatants of sample tissue homogenates. In brief, microplates were coated with 100 μ l/well of capture antibody, and then they were incubated overnight at 4°C. After washes, the plates were blocked with assay diluent at room temperature (RT) for 1 hour. One hundred microliters of a serum sample was added to each well of the plate, followed by incubation for 2 hours at room temperature (RT). Working detector was added into each well, and the plate was incubated for an additional 1 hour at RT before the addition of substrate solution. The reaction was stopped by adding stop solution. The absorbance was read using the ELISA reader. The concentrations were calculated from standard curve according to the instructions in the protocol.

Nitric Oxide Determination

Nitric oxide (NO) level in tumor tissues was determined colorimetrically as nitrite by Griess reaction.¹³

Measurement of Radical-Scavenging Ability in Hepatic Tissue Using Electron Spin Resonance Spectroscopy

The liver tissues were quickly removed from mice and were gently lyophilized and were evaporated to dryness under vacuum. All samples were dissolved in a small volume of toluene, and were transferred to a round ESR cell. The cells were capped with a rubber septum and were thoroughly deoxygenated by nitrogen bubbling before ESR spectroscopy was performed. The ESR spectra were recorded at room temperature using a Bruker EPR ER-200D spectrometer, and spectral accumulation was done by using a Bruker ER-140 ASPECT 2000) data system. The microwave power was 2 mW, the modulation amplitude was 1 G and 1 E4 receiver gain. The response time constant was 10 ms, with a field-sweeping rate of 100 G/42 seconds. The height of powder sample inside the quartz tube was about 10 mm. ESR spectral analyses were performed through the use of a computer simulation program.¹⁴

Histopathological Study

Autopsy samples were taken from the thigh muscle of mice in different groups and fixed in 10% formal saline for

24 hours. Washing was done in tap water, then serial dilutions of alcohol (methyl, ethyl, and absolute ethyl) were used for dehydration. Specimens were cleared in xylene and embedded in paraffin at 56° in a hot air oven for 24 hours. Paraffin beeswax tissue blocks were prepared for sectioning at 4 μ m thickness by sledge microtome. The obtained tissue sections were collected on glass slides, deparaffinized, and stained by hematoxylin and eosin stain for routine examination through the light electric microscope.¹⁵

Statistical Analysis

Survival data were analyzed using Kaplan-Meier curves and compared by Mantel-Cox (Log Rank) and Gehan-Breslow-Wilcoxon statistics. The data were expressed as mean \pm SEM. Data normality was verified by Kolmogorov-Smirnov (KS, $P > .1$). Statistical analysis was conducted using 1-way analysis of variance (ANOVA), followed by Tukey-Kramer post hoc multiple comparisons among treatment means. Statistical analyses were performed using Prism, version 6 (GraphPad Software, La Jolla, CA). All tests were 2-tailed, and p values $< .05$ were considered statistically significant.

Result

Impact of Chrysin and/or γ -Irradiation Exposure on Tumor Volume in Different Mice Groups

Figure 1 demonstrates that the size of solid EAC tumors reached 6500.40 mm³ 7 days from when the tumor reached 1 cm³ during the experimental period, and enlarged to 38700.46 mm³ at the end of the experiment. A gradual significant decrease in the tumor size during treatment of EAC-bearing mice with Ch, was demonstrated, compared to untreated EAC-bearing mice. On the other hand, exposure of EAC-bearing mice to γ -irradiation produced a marked significant reduction in the tumor size, and a radiosensitizing effect was observed in decreasing the tumor size of γ -irradiated-EAC-bearing mice co-administered with Ch.

Effect of Ch Administration and/or γ -Irradiation Exposure to Mice on TNF- α Expression

The data obtained from the present study showed that the expression of TNF- α in tumor tissue was significantly amplified compared with the normal control group (Figure 2). The TNF- α expression in the EAC group enlarged significantly ($P < .05$) by 96.2-fold when compared with the respective normal controls. We observed significant changes in TNF- α response in the current study when EAC mice were injected with chrysin, wherein the group of EAC + Ch, manifested a considerable amelioration by a significant decline ($P < .05$) in TNF- α expression level (40.9%),

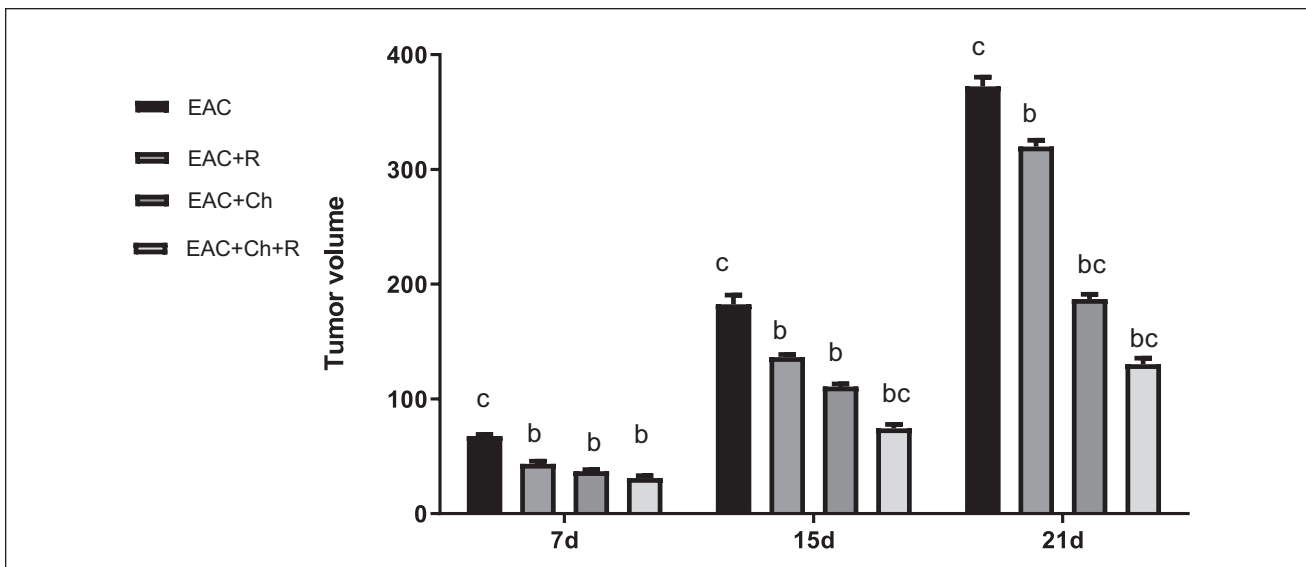


Figure 1. The effect of chrysin treatment and/or γ -irradiation on tumor volume. Abbreviations: EAC: Ehrlich solid tumor; R: radiation; Ch: chrysin; b: significantly different from EAC; c: significantly different from EAC + R. Each value represents the mean \pm SE (n=6).

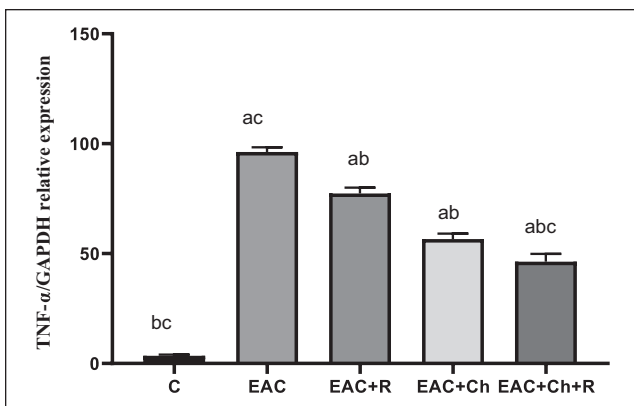


Figure 2. A histogram showing the effect of exposure to γ -radiation and/or treatment with chrysin on TNF- α expression. Abbreviations: C: control; EAC: Ehrlich solid tumor; R: radiation; Ch: chrysin; a: significantly different from control; b: significantly different from EAC; c: significantly different from EAC + R. Each value represents the mean \pm SE (n=6).

associated with a significant downregulation in TNF- α expression level in the EAC + Ch + R group by (41%) compared with the irradiated mice bearing solid tumor group (EAC + R).

Influence of Ch Administration and/or γ -Irradiation Exposure to Mice on Nitric Oxide Concentration

The data obtained from the present study showed that the concentration of NO in tumor tissue significantly increased

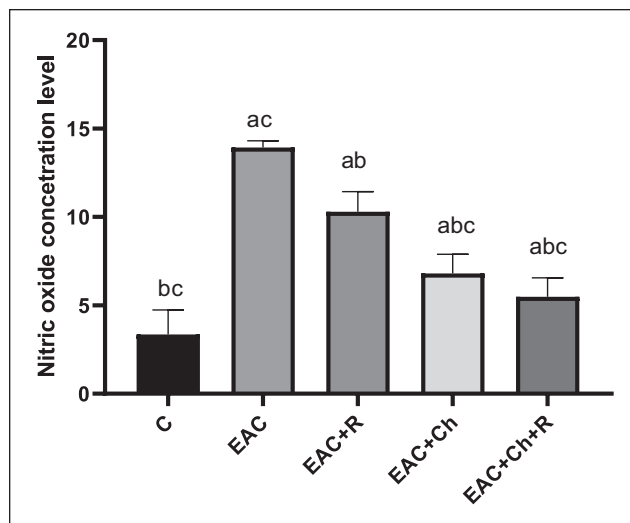


Figure 3. A histogram showing nitric oxide concentration in the right thigh muscle (control) or tumor tissue in different groups. Abbreviations: C: control; EAC: Ehrlich solid tumor; R: radiation; Ch: chrysin; a: significantly different from control; b: significantly different from EAC; c: significantly different from EAC + R. Each value represents the mean \pm SE (n=6).

compared with the normal control group (Figure 3). The NO concentration in the EAC group was significantly enlarged ($P < .05$) by (4.6-fold), when compared with the normal control. On the other hand, a substantial deterioration ($P < .05$) in NO concentration level was seen in the EAC + Ch + R group by (48%) compared with the irradiated EAC group (EAC + R).

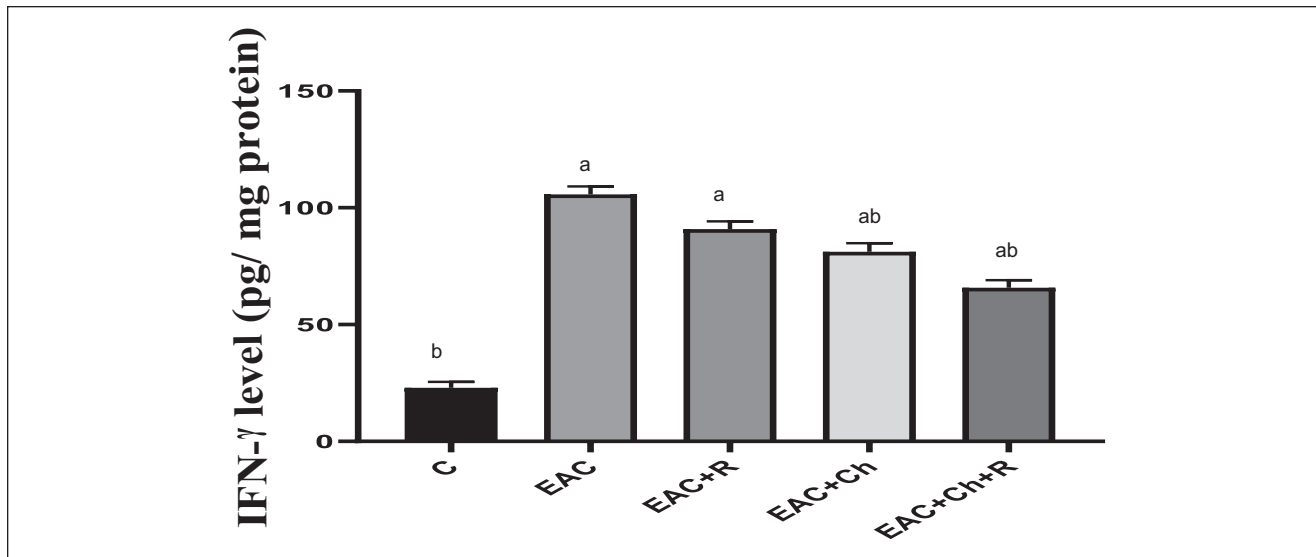


Figure 4. Interferon gamma concentration (IFN- γ) in the right thigh muscle or tumor tissue in different groups. Abbreviations: C: control; EAC: Ehrlich solid tumor; R: radiation; Ch: chrysin; a: significantly different from control; b: significantly different from EAC. Each value represents the mean \pm SE (n=6).

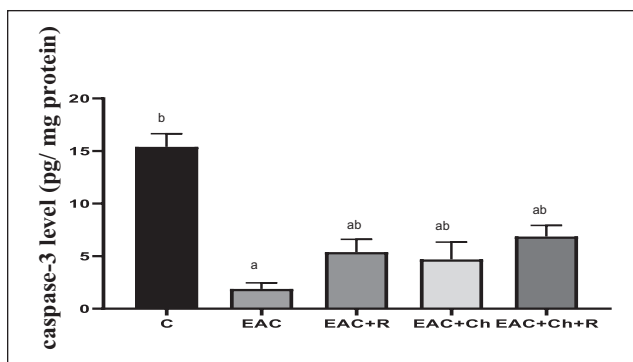


Figure 5. Effect of chrysin and/or γ -irradiation exposure on caspase-3 levels in the right thigh muscle or tumor tissue in different groups. Abbreviations: C: control; EAC: Ehrlich solid tumor; R: radiation; Ch: chrysin; a: significantly different from control; b: significantly different from EAC. Each value represents the mean \pm SE (n=6).

Impact of Ch Administration and/or γ -Irradiation Exposure to Mice on Caspase-3, IFN- γ Levels

Figures 4 and 5 showed that mice bearing solid EAC tumors manifested significant amelioration of IFN- γ and caspase-3 levels respectively, where IFN- γ was significantly increased by 4.6-fold and caspase-3 was meaningfully decreased by 87% compared to non-EAC bearing mice. Treatment of EAC-bearing mice with Ch resulted in a pronounced decline in IFN- γ activity and elevation in caspase-3 level respectively, compared to untreated EAC-bearing mice. On the other hand, exposure of EAC-bearing mice to γ -irradiation either alone or in combination with Ch treatment produced

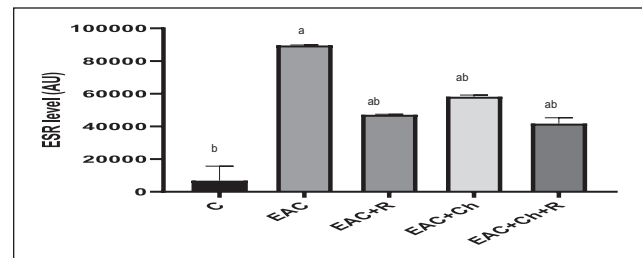


Figure 6. Statistical analysis for the peak intensity for liver tissue ESR free radical in different groups. Abbreviations: C: control; EAC: Ehrlich solid tumor; R: radiation; Ch: chrysin; a: significantly different from control; b: significantly different from EAC. Each value represents the mean \pm SE (n=6).

a significant sharp decrease in IFN- γ and upsurge in caspase-3 levels respectively, compared to untreated EAC-bearing mice.

The Effect of Liver Tissue ESR Free Radical in Different Groups

Figure 6 showed that mice bearing solid EAC tumors manifested high significant increases in the free radical peak intensity, compared to non EAC-bearing mice. Treatment of EAC-bearing mice with Ch resulted in a pronounced decline in free radical peak intensity, compared to untreated EAC-bearing mice. On the other hand, exposure of EAC-bearing mice to γ -irradiation either alone or in combination with Ch treatment produced a significant sharp decrease in free radical peak intensity, compared to untreated EAC-bearing mice.

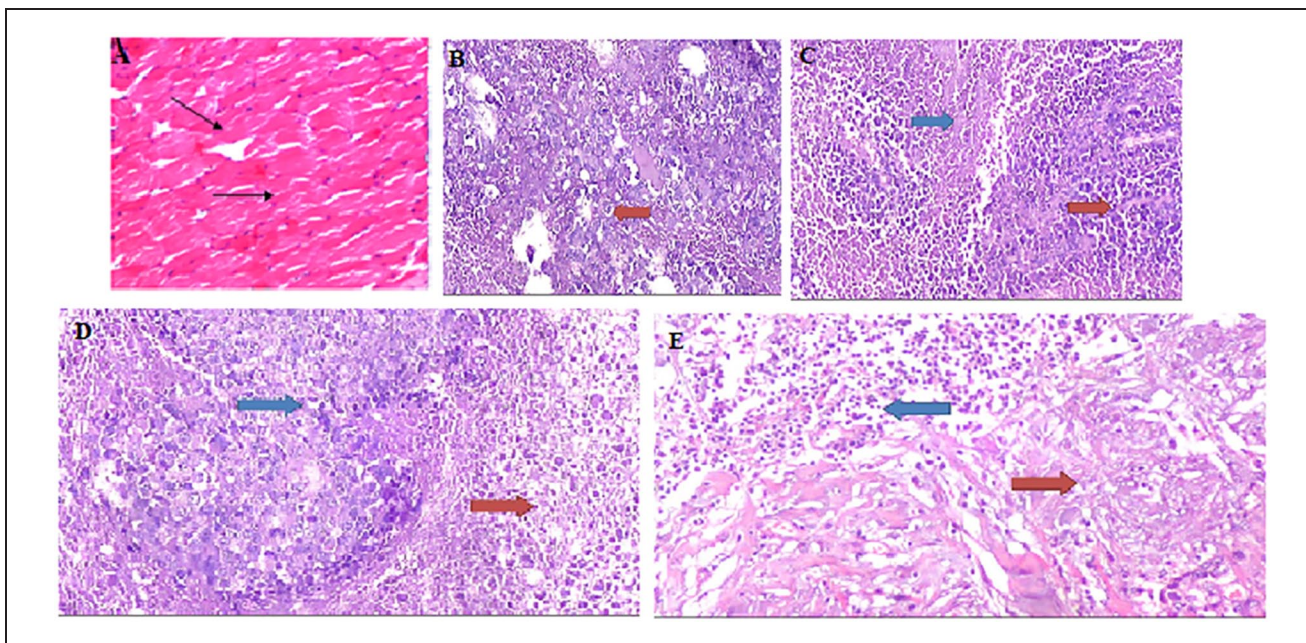


Figure 7. Photomicrograph sections of right thigh muscles. (A) Normal control; C displayed normal histological structure of striated bundles (→). (B) Mice bearing solid tumor; EAC Ehrlich tumor cells exhibiting pleomorphism, hyperchromatism (*), infiltrating and penetrating the muscle bundles, and aggregated in focal manner in between (→). (C) Chrysin showed malignant cells (red arrow) surrounded by 10% of tumor necrosis (blue arrow). (D) Irradiated mice bearing solid tumor; EAC + R showed malignant cells (blue arrow) surrounded by 20% of tumor necrosis (red arrow). (E) Irradiated mice bearing solid tumor treated with chrysin; EAC + ch + R showed dead cells (red arrow) and necrotic cells (blue arrow) after Ch administration and/or gamma radiation.

Influence of Ch Treatment on Histopathology of EAC-Bearing Mice Irradiated or Not Irradiated

Photomicrographic examinations of control mice thigh muscle tissue demonstrate normal histological structure of striated bundles (Figure 7A). However, photomicrographs of EAC mice displayed compactness of the tumor cells scattered within the muscular tissues and aggregated in a focal manner, infiltrating and penetrating the muscle bundles. Groups of large round and polygonal cells with pleomorphic shapes, hyperchromatic nuclei and binucleation, several degrees of cellular and nuclear pleomorphism were observed (Figure 7B). Further, in mice exposed to whole body gamma radiation, a focal area of aggregated intact Ehrlich tumor cells appeared rather than musculature necrosis in other sides (Figure 7D). On the other hand, the histopathological investigation performed showed a great destruction of tumor tissue represented by the appearance of dead and necrotic cells after Ch administration (Figure 7C) and or gamma radiation (Figure 7E).

Discussion

Cancer is anticipated to be the largest cause of death and a major impediment to increasing life expectancy in this century; according to 2018 forecasts, there will be over 18million new cancer diagnoses with a mortality rate of

over 50%. Because the immune system plays such an important role in cancer formation, researchers have attempted to develop tumor-targeted immunotherapies with the goal of enhancing the antitumor immune response and, as a result, eradicating the neoplasia in progress.¹⁶ Patients with many tumor types benefit significantly from cancer immunotherapy, which can result in full tumor eradication in rare situations.¹⁷

In an attempt to improve cancer therapeutic protocols, this study was undertaken to evaluate the antitumor effect of chrysin together with γ -irradiation against solid EAC tumors in female mice. Different molecular targets were analyzed in order to explore the suppressive effect of chrysin on the growth of solid tumors.

In this study, a significant upregulation was recorded in IFN- γ activity and TNF- α messenger RNA (mRNA) expression in solid EAC tumors, compared to non- EAC-bearing mice (Figures 2 and 4). Certain cytokines, such as TNF- α and IFN- γ , are key factors in determining the contribution of the inflammatory process to cancer.¹⁸ IFN- γ has a lengthy history of being used as a pro-tumor factor. It stimulates other immuno-suppressive pathways by allowing the creation of immune checkpoint inhibitory molecules and indoleamine-2,3-dioxygenase (IDO).¹⁹ IFN- γ acts as an opponent of the immune system through immunosuppression, angiogenesis, and tumor cell proliferation. Its effect on tumors is mediated through induction of PDL1, IDO1,

iNOS, FAS, and FASL expression. Prevention of IFN γ signaling decreased PDL1 expression by tumor cells and increased IFN γ -responsive gene expression by immune cells, including exhausted T cells.¹⁷ One common theme that shows the pro-tumorigenic effects of IFN- γ is that tumors that are exposed to IFN- γ show greater immunoevasive capabilities. For example, several IFN- γ pathway target genes are known to be involved in immunosuppressive and immunoevasive mechanisms that are geared toward suppression of CTL- and NK cell-mediated antitumor immune responses.²⁰ TNF- α acts as an autocrine growth factor for tumor angiogenesis by inducing numerous alterations in endothelial cell gene expression, including activation of adhesion molecules, integrins, and MMPs.²¹ TNF- α is a crucial factor in tumor metastasis. In tumor microenvironment endothelial cells, it enhances the expression of fibroblast growth factor (bFGF), interleukin-8 (IL-8), and vascular endothelial growth factor (VEGF).²² TNF- α binds to 2 receptors, TNFR1 and TNFR2, and exerts its actions. TNFR1 is found in all cell types and is widely expressed. TNFR1 activation can trigger cell survival pathways. The concentration of TNF- α in the microenvironment, as well as the actions of other relevant cytokines, are used to regulate the receptor's final downstream activity.²³ TNFR2 is mostly present on immune cells, where TNF- α activates its pathway, which aids in the regulation of immune response and inflammation. The activation of TNFR2 on immune cells in the TME as well as cancer cells can promote tumor development and progression.²⁴ Increased TNFR2 expression found on regulatory T cells within the TME can suppress the immune response and prevent activation of cytotoxic T cells, which decreases the ability of the immune response to suppress the tumor.²³ TNF- α can suppress the myeloid-derived suppressor (MDSC) differentiation and induce accumulation of MDSC, which enhances their immunosuppressive effects in the TME through TNFR2 signaling.^{23,25}

Further, the significant increase ($P < .05$) in NO concentration of EAC-bearing mice might be due to TNF- α over-expression. Our results are in line with Zhang and Xu,²⁶ who demonstrated the role of NO in tumor progression via disrupting the host immune system to allow for tumor cell escape from immune surveillance. Jadeski et al. determined that NO-mediated tumor growth and metastasis of the C3H/HeJ mammary tumor cell line acts via the sequential activation of nitric oxide synthase (NOS), guanylate cyclase (GC), and mitogen-activated protein kinase (MAPK) pathways.^{27,28} The production of nitric oxide (NO) is a key feature of immunosuppressive myeloid cells, which impair T cell activation and proliferation via reversibly blocking interleukin-2 receptor signaling.²⁹

It has been demonstrated that TNF- α is a mediator of NO synthesis.³⁰ Nitric oxide synthase (NOS) comprises a family of enzymes that can generate NO. The 3 isoforms of

NOS include neuronal NOS (nNOS), inducible NOS (iNOS), and endothelial NOS (eNOS) that are encoded by the NOS1, NOS2, and NOS3 genes, respectively. iNOS is the most widely studied isoform due to its significant and contrasting roles in cancer.³¹ iNOS expression is regulated at the transcriptional level by cytokines (IFN γ , IL-1 β , and TNF- α), bacterial endotoxins, and oxidative stress/hypoxia.²⁸ Nitric oxide is a diatomic free radical molecule with high reactivity. High output of nitric oxide leads to nitration, nitrosation, and oxidation, which can then affect cellular functioning. NO can interact with oxygen or oxide ions to form reactive nitrogen species such as dinitrogen trioxide and peroxynitrite, cause DNA damage through nitrosative and oxidative stress. Peroxynitrites can oxidize and nitrate DNA and also potentially cause single-strand DNA breaks due to an attack on the sugar-phosphate backbone.³²

The disturbance in the angiogenic and apoptotic regulators leads to tumor proliferation and growth, which was clearly demonstrated by the increase in EAC tumor volume as shown in Figure 1. Neovascularization enhances the ability of the tumor to grow and increases its invasiveness and metastatic ability.³³ In order to progress, cancers need to circumvent immune control. This was nicely illustrated by a study of carcinogen-induced cancers that arose in immune deficient versus immune sufficient mice. Cancers from immune deficient mice grew when transplanted into other immune deficient mice. However, these same cancers were generally rejected in wild type mice, showing that they were inherently immunogenic.³⁴ In contrast, tumors that arose in wild type mice would often grow when transplanted into other wild type mice. These findings indicated that tumors that arose in the presence of the intact immune system in wild type mice evolved in ways that allowed them to evade immune elimination.³⁵

Apoptosis is a programmed cell death that maintains the stability of the internal environment through removing genetic mutations and unstable cells. However, this process is inhibited in cancer which leads to the accumulation of various genetically unstable cells. Our results demonstrated a significant decline in the level of apoptotic molecule (caspase-3) in the solid EAC tumors, compared to non-EAC bearing mice (Figure 5). Caspases have important roles in various diseases and it has been shown that caspase deficiency results in tumor development.³⁶ Caspase-3 mediated apoptosis is a major focus in the field of cancer growth inhibition, because activation of the proteolytic caspase cascade is a critical component in the execution of apoptotic cell death.³⁷ The increase in TNF- α expression is accompanied with a decrease in caspase-3 activities. These findings are in line with Zhang et al³⁸ who found that knockdown of transmembrane TNF- α expression enhances the therapeutic efficacy of doxorubicin in a xenograft mouse model where the combination of tmTNF- α inhibition and DOX treatment

resulted in much more pronounced suppression of tumor growth.

Additionally, the free radical level was elevated in liver tissue of EAC mice (Figure 6). The presence of tumor in the human body or in experimental animals could affect many functions of vital organs in the body, even when the site of tumor does not interfere directly with this function. Gonenc et al³⁹ reported that enlargement in tumor size might cause antioxidant disturbances and oxidative stress elevation in vital organs of the tumor host. The disturbance in redox tone in normal cells could be attributed to influx of certain cytokines released from proximal tumor cells. A noticeable alteration in muscle bundles and the cellular architecture in addition to the occurrence of tumor cell infiltration and penetration in micrographs of EAC and EAC + R when matched with the micrograph of normal control thigh muscle bundles (Figure 7). Elbakary et al¹⁰ attributed these changes to the alteration in biochemistry of tumor where the changes in TNF- α signaling and the accumulation of MDA in the cells of muscle bundles destroyed the cellular integrity and enhanced tumor proliferation. The current data revealed that the upregulation of TNF- α genes and induction of IFN- γ activity and NO concentration along with apoptosis suppression in solid EAC-bearing mice collectively enhance tumor cell proliferation and neovascularization, which ultimately resulted in the acceleration of tumor growth, invasiveness, and metastatic ability of tumor cells.

Exposure of EAC-bearing mice to γ -irradiation produced a significant delay in tumor volume, which was achieved through the induction of apoptosis. Radiation-induced DNA damage activates a variety of signaling pathways; the intrinsic apoptotic pathway has been considered the primary mechanism mediating ionizing radiation-induced apoptosis, making tumor cells unable to divide and grow.⁴⁰⁻⁴² Many cancer cells, including lung, prostate, immortalized keratinocytes, and colon cancer cells, are committed to apoptotic cell death when exposed to radiation.^{43,44} Immunotherapy plays increasingly important roles during tumor treatment, especially in assisting radiotherapy (RT) to improve clinical outcomes.²⁹ Experimental data indicated that immune responses activated by RT could be impeded by production of NO. L-n6-(1-iminoethyl)-lysine (L-NIL), as a potent iNOS inhibitor, enhanced RT susceptibility of treatment-refractory head and neck cancer.⁴⁵ Moreover, NO reduction with a highly-selective NOS inhibitor, NG-monomethyl-L-arginine monoacetate (LNMMMA), enhanced the radiosensitization of nonsmall cell lung cancer (NSCLC) cells.⁴⁶ Xu et al²⁹ found that RT could effectively inhibit immune system activation and promoted T cell function via suppressing NO synthesis in immunosuppressive myeloid cells, thereby further enhancing the efficacy and clinical outcomes of RT.

Currently, surgical resection, radiation, and chemotherapy are common therapeutic strategies used to fight against

cancer. However, surgery and the current combination chemotherapy options are limited by the side effects associated with treatment and by some tumor cells eventually developing drug resistance.⁴⁷ Therefore, it is imperative to develop novel strategies to overcome cancer, including therapies that can be applied in combination with current strategies. Mounting evidence indicates that natural compounds provide a new window of opportunity due to their safety and potential to overcome resistance to chemotherapy.

The result of this study revealed that treatment of EAC-bearing mice with Ch significantly reduced the growth of solid tumors, and a synergistic effect was demonstrated following combination with γ -irradiation. As a key player in tumor proliferation, angiogenesis, and inflammatory cascade induction, the down regulation of TNF- α expression following treatment of irradiated and non-irradiated EAC-bearing mice with Ch reduced tumor growth via multiple mechanisms, including suppression of tumor cell proliferation (reduction in tumor volume), angiogenesis (down regulation of tumor TNF- α expression and NO concentration), and enhancing apoptosis (induction of tumor caspase-3). Where the inducible form of nitric oxide synthase is expressed mainly through TNF- α activated pathway,⁴⁸ so TNF- α is the maestro for controlling the angiogenesis process. Ch has demonstrated potential efficacy in inhibiting TNF- α and NO concentration.⁴⁹

Our result are in line with Hermenean et al⁵⁰ who found that the increase in hepatic tumor necrosis factor- α (TNF- α) protein expression in carbon tetrachloride (CCl₄)-induced acute liver damage was significantly decreased in the livers of mice pre-treated with chrysin. Chrysin suppresses inflammation; it suppressed the levels of IFN- γ , NO, IL-1 β , and TNF- α expression through inhibition of NF- κ B signaling. NF- κ B is a vital nuclear transcription factor for inflammation and regulates the transcription of several inflammatory mediators. It has 5 subunits: p50, p52, p65, Rel, and Rel-B. In the inactive state, these subunits dimerize and bind I κ B α . When cells receive stimuli, the dimers (p65-p50 or c-Rel-p50 heterodimers) are released from I κ B α and act as the functional form of NF- κ B. Functional NF- κ B activated macrophages secreting TNF- α , IFN- γ , iNOS, and IL-1 β can induce tissue damage. It was observed that chrysin suppressed the expression of p65. Therefore, the translocation of activated NF- κ Bp65 to the nucleus may be downregulated in this situation, thus restricting the expression of TNF- α , IFN- γ , iNOS, and IL-1 β .⁵¹ Encountering of cancer cells with chrysin resulted in DNA damage and prompted mitochondrial membrane agitation going along with downregulation of Bcl-2, activation of BID and Bax, cytochrome c release, and caspase-3-mediated apoptosis. ROS production by chrysin was the critical mediator behind induction of ER stress, leading to JNK phosphorylation, intracellular Ca²⁺ release, and activation of the mitochondrial apoptosis pathway.²

In many studies chrysin has been shown to exert beneficial pharmacological activities: it suppressed pro-inflammatory cytokine expression and histamine release; downregulated nuclear factor kappa B (NF- κ B), cyclooxygenase 2 (COX-2), and inducible nitric oxide synthase (iNOS); upregulated apoptotic pathways; inhibited angiogenesis and metastasis formation, protecting from cancer; suppressed DNA topoisomerases and histone deacetylase; downregulated tumor necrosis factor α (TNF- α) and interleukin 1 β (IL-1 β); and promoted protective signaling pathways in the heart, kidney, and brain.^{2,52,53}

Recently, radiation technology has been applied to enhance the biological properties or physical characteristics of various biomolecules through structural modification, some molecules transformed through gamma irradiation exhibit improved physiological properties.^{54,55}

The results of our study were paralleled with the findings of Song et al⁵⁶ who found that the anticancer effect of chrysin was enhanced upon exposure to gamma irradiation. Gamma irradiation induces the production of new radiolytic peaks simultaneously with the decrease of the chrysin peak, which increases the cytotoxicity in HT-29 human colon cancer cells. An irradiated chrysin exhibited a stronger apoptotic effect in HT-29 cells than intact chrysin. The apoptotic characteristics induced by irradiated chrysin in HT29 cells was mediated through the intrinsic signaling pathway, including the excessive production of included reactive oxygen species, the dissipation of the mitochondrial membrane potential, regulation of the B cell lymphoma-2 family, activation of caspases-9 and 3, and cleavage of poly (adenosine diphosphate-ribose) polymerase.^{57,58} The structural transformation is initiated by CH₂OH radical derived from gamma irradiation. There is one possible mechanism; the radical reacts with chrysin molecule and induces cleavage of the C=O bond in the A ring. The C=O double bond in the A ring was recovered by taking away a hydrogen atom from C8, The remaining CH₂OH radicals react with C8, which forms a hydroxyethyl derivative of chrysin. Some previous studies proposed that hydroxyethyl derivatives exhibited stronger anticancer activity.^{59,60}

Further, the results of histological examination for the tumor micrograph of EAC + Ch and EAC + Ch + R mice groups compared to EAC mice reveals noticeable amelioration in cell architecture of the muscle bundle in addition to certain improvement in the state of tumor cell infiltration, penetration and area of necrosis, and enhancing tumor cells apoptosis (Figure 7). The results give the impression that Ch plays an efficient role in the inhibition of the TNF- α and IFN- γ activation event. It displays anti-proliferative and anti-angiogenic activity against cancer cells in vivo.² A pharmaceutical study of Gao et al. showed that chrysin absorption is moderate due to its low solubility and moderate permeability. Low bioavailability is the challenge for

developing chrysin as a therapeutic drug.⁶¹ A suggestion for future clinical study is to administering chrysin in certain formulations (eg, nano-particles) that can enhance its oral bioavailability, which should be considered to evaluate its in vivo efficacy more appropriately.

In conclusion, treatment of E, E + R groups with Ch exerted a marked effect in the retardation of tumor growth as compared to tumor bearing mice group. These observations could be attributed to the immune stimulating, antiapoptotic, and antioxidant capacity of Ch. Taking everything into account, our study agrees with the fact that natural products are versatile compounds in cancer therapy due to their capacity in targeting various molecular pathways.

Acknowledgments

Thanks to all the authors.

Declaration of Conflicting Interests

The author(s) declared no potential conflicts of interest with respect to the research, authorship, and/or publication of this article.

Funding

The author(s) received no financial support for the research, authorship, and/or publication of this article.

Ethics statement

This study was conducted in accordance with the recommendations in the Guide for the Use and Care of Laboratory Animals of the National Institute of Health (NIH no. 85:23, revised 1996) and in compliance with the regulations of Ethical Committee (REC) of the National Center for Radiation Research and Technology (NCRRT), Atomic Energy Authority, Cairo, Egypt (Approval No: 28A/21). REC has approved this research protocol, following the 3Rs principles for animal experimentation (Replace, Reduce, and Refine) and is organized and operated according to the CIOMS and ICLAS International Guiding Principles for Biomedical Research Involving Animals 2012.

ORCID iD

Nermeen M. El Bakary  <https://orcid.org/0000-0002-0128-3159>

References

1. Moghadam ER, Ang HL, Asnaf SE, et al. Broad-spectrum preclinical antitumor activity of chrysin: current trends and future perspectives. *Biomolecules*. 2020;10:1374.
2. Talebi M, Talebi M, Farkhondeh T, et al. Emerging cellular and molecular mechanisms underlying anticancer indications of chrysin. *Cancer Cell Int*. 2021;21:214.
3. Forma E, Bryś M. Anticancer activity of propolis and its compounds. *Nutrients*. 2021;13:2594.
4. El Bakary NM. Immune stimulation and proapoptotic effect of honey bee propolis against solid ehrlich carcinoma bearing mice. *Int J Clin Stud Med Case Rep*. 2021;9:1-6.

5. Martinello M, Mutinelli F. Antioxidant activity in bee products: a review. *Antioxidants*. 2021;10:71.
6. El Bakary NM, Azab K, Hanafy SM, Abdul Aziz GM, Fayed AM. Calcitriol revises aromatase gene expression in Ehrlich solid tumor bearing mice exposed to low dose gamma radiation. *J Cancer Res Cell Ther*. 2021;5:1-9.
7. Feinendegen LE. Evidence for beneficial low level radiation effects and radiation hormesis. *Br J Radiol*. 2005;78:3-7.
8. Calabrese EJ, Baldwin LA. Scientific foundations of hormesis. *Crit Rev Toxicol*. 2001;31:351-624.
9. Villar IC, Jiménez R, Galisteo M, Garcia-Saura MF, Zarzuelo A, Duarte J. Effects of chronic chrysin treatment in spontaneously hypertensive rats. *Planta Med*. 2002;68:847-850.
10. El Bakary NM, Alsharkawy AZ, Shouaib ZA, Barakat EMS. Role of bee venom and melittin on restraining angiogenesis and metastasis in γ -irradiated solid Ehrlich carcinoma-bearing mice. *Integr Cancer Ther*. 2020;19:153473542 0944476.
11. Papadopoulos D, Kimler BF, Estes NC, et al. Growth delay effect of combined interstitial hyperthermia and brachytherapy in a rat solid tumor model. *Anticancer Res*. 1989;9:45-47.
12. Livak KJ, Schmittgen TD. Analysis of relative gene expression data using real-time quantitative PCR and the $2^{-\Delta\Delta CT}$ method. *Methods*. 2001;25:402-408.
13. Miranda KM, Espey MG, Wink DA. A rapid simple spectrophotometric method for simultaneous detection of nitrate and nitrite. *Nitric Oxide*. 2001;5:62-71.
14. Oehler UM, Janzen EG. Simulation of isotropic electron spin resonance spectra: a transportable basic program. *Can J Chem*. 1982;60:1542-1548.
15. Bancroft JD, Stevens A, Dawswon MP. *Theory and Practice of Histological Techniques*. 4th ed. Churchill Livingstone; 1996:273-292.
16. Celińska-Janowicz K, Zaręba I, Lazarek U, et al. Constituents of propolis: chrysin, caffeic acid, p-coumaric acid, and ferulic acid induce PRODH/POX-dependent apoptosis in human tongue squamous cell carcinoma cell (CAL-27). *Front Pharmacol*. 2018;9:336.
17. Gocher AM, Workman CJ, Vignali DAA. Interferon- γ : teammate or opponent in the tumour microenvironment? *Nat Rev Immunol*. 2022;22:158-172.
18. Kobelt D, Zhang C, Clayton-Lucey IA, et al. Pro-inflammatory TNF- α and IFN- γ promote tumor growth and metastasis via induction of MACC1. *Front Immunol*. 2020;11:980.
19. Jorgovanovic D, Song M, Wang L, Zhang Y. Roles of IFN- γ in tumor progression and regression: a review. *Biomark Res*. 2020;8:49.
20. RazaZaid M. The interferon-gamma paradox in cancer. *J Interferon Cytokine Res*. 2019;39:30-38.
21. Song K, Zhu F, Zhang HZ, Shang ZJ. Tumor necrosis factor- α enhanced fusions between oral squamous cell carcinoma cells and endothelial cells via VCAM-1/VLA-4 pathway. *Exp Cell Res*. 2012;318:1707-1715.
22. Wagener FA, Feldman E, de Witte T, Abraham NG. Heme induces the expression of adhesion molecules ICAM-1, VCAM-1, and E selectin in vascular endothelial cells. *Proc Soc Exp Biol Med*. 1997;216:456-463.
23. Laha D, Grant R, Mishra P, Nilubol N. The role of tumor necrosis factor in manipulating the immunological response of tumor microenvironment. *Front Immunol*. 2021;12:656908.
24. Sheng Y, Li F, Qin Z. TNF receptor 2 makes tumor necrosis factor a friend of tumors. *Front Immunol*. 2018;9:1170.
25. Sade-Feldman M, Kanterman J, Ish-Shalom E, Elnekave M, Horwitz E, Baniyash M. Tumor necrosis factor- α blocks differentiation and enhances suppressive activity of immature myeloid cells during chronic inflammation. *Immunity*. 2013;38:541-554.
26. Zhang XM, Xu Q. Metastatic melanoma cells escape from immunosurveillance through the novel mechanism of releasing nitric oxide to induce dysfunction of immunocytes. *Melanoma Res*. 2001;11:559-567.
27. Jadeski LC, Chakraborty C, Lala PK. Nitric oxide-mediated promotion of mammary tumour cell migration requires sequential activation of nitric oxide synthase, guanylate cyclase and mitogen-activated protein kinase. *Int J Cancer*. 2003;106:496-504.
28. Navasardyan I, Bonavida B. Regulation of T cells in cancer by nitric oxide. *Cells*. 2021;10:2655.
29. Xu J, Luo Y, Yuan C, et al. Downregulation of nitric oxide collaborated with radiotherapy to promote anti-tumor immune response via inducing CD8+ T cell infiltration. *Int J Biol Sci*. 2020;16:1563-1574.
30. Liu JG, Zhao HJ, Liu YJ, Wang XL. Effect of selenium-enriched malt on VEGF and several relevant angiogenic cytokines in diethylnitrosamine-induced hepatocarcinoma rats. *J Trace Elem Med Biol*. 2010;24:52-57.
31. Liao W, Ye T, Liu H. Prognostic value of inducible nitric oxide synthase (iNOS) in human cancer: a systematic review and meta-analysis. *Biomed Res Int*. 2019;2019:6304851.
32. Mintz J, Vedenko A, Rosete O, et al. Current advances of nitric oxide in cancer and anticancer therapeutics. *Vaccines*. 2021;9:94.
33. Dhankhar R, Dahiya K, Singh V, Sangwan L, Kaushal V. Nitric oxide and cancer. *J Clin Diagn Res*. 2010;4:2550-2559.
34. Shankaran V, Ikeda H, Bruce AT, et al. IFN γ and lymphocytes prevent primary tumour development and shape tumour immunogenicity. *Nature*. 2001;410:1107-1111.
35. Koebel CM, Vermi W, Swann JB, et al. Adaptive immunity maintains occult cancer in an equilibrium state. *Nature*. 2007;450:903-907.
36. Rahmanian N, Hosseinimehr SJ, Khalaj A. The paradox role of caspase cascade in ionizing radiation therapy. *J Biomed Sci*. 2016;23:88.
37. Yadav P, Yadav R, Jain S, Vaidya A. Caspase-3: a primary target for natural and synthetic compounds for cancer therapy. *Chem Biol Drug Des*. 2021;98:144-165.
38. Zhang Z, Lin G, Yan Y, et al. Transmembrane TNF-alpha promotes chemoresistance in breast cancer cells. *Oncogene*. 2018;37:3456-3470.
39. Gönenç A, Ozkan Y, Torun M, Simşek B. Plasma malondialdehyde (MDA) levels in breast and lung cancer patients. *J Clin Pharm Ther*. 2001;26:141-144.
40. Xiao M, Whitnall MH. Pharmacological countermeasures for the acute radiation syndrome. *Curr Mol Pharmacol*. 2009;2:122-133.

41. Panganiban RA, Snow AL, Day RM. Mechanisms of radiation toxicity in transformed and non-transformed cells. *Int J Mol Sci*. 2013;14:15931-15958.
42. Medhat AM, Azab KS, Said MM, El Fatih NM, El Bakary NM. Antitumor and radiosensitizing synergistic effects of apigenin and cryptotanshinone against solid Ehrlich carcinoma in female mice. *Tumour Biol*. 2017;39:1010428317728480.
43. Petit- Frère C, Capulas E, Lyon DA, et al. Apoptosis and cytokine release induced by ionizing or ultraviolet B radiation in primary and immortalized human keratinocytes. *Carcinogenesis*. 2000;21:1087-1095.
44. Rödel C, Haas J, Groth A, Grabenbauer GG, Sauer R, Rödel F. Spontaneous and radiation-induced apoptosis in colorectal carcinoma cells with different intrinsic radiosensitivities: survivin as a radioresistance factor. *Int J Radiat Oncol Biol Phys*. 2003;55:1341-1347.
45. Newton JM, Hanoteau A, Liu HC, et al. Immune microenvironment modulation unmasks therapeutic benefit of radiotherapy and checkpoint inhibition. *J Immunother Cancer*. 2019;7:216.
46. Saleem W, Suzuki Y, Mobaraki A, et al. Reduction of nitric oxide level enhances the radiosensitivity of hypoxic non-small cell lung cancer. *Cancer Sci*. 2011;102:2150-2156.
47. Xu Y, Tong Y, Ying J, et al. Chrysin induces cell growth arrest, apoptosis, and ER stress and inhibits the activation of STAT3 through the generation of ROS in bladder cancer cells. *Oncol Lett*. 2018;15:9117-9125.
48. Azab KSH, Mostafa AH, Ali EM, Abdel-Aziz MA. Cinnamon extract ameliorates ionizing radiation-induced cellular injury in rats. *Ecotoxicol Environ Saf*. 2011;74:2324-2329.
49. Chang H, Wang Y, Yin X, Liu X, Xuan H. Ethanol extract of propolis and its constituent caffeic acid phenethyl ester inhibit breast cancer cells proliferation in inflammatory microenvironment by inhibiting TLR4 signal pathway and inducing apoptosis and autophagy. *BMC Complement Altern Med*. 2017;17:471.
50. Hermenean A, Mariasiu T, Navarro-González I, et al. Hepatoprotective activity of chrysin is mediated through TNF- α in chemically-induced acute liver damage: an *in vivo* study and molecular modeling. *Exp Ther Med*. 2017;13:1671-1680.
51. Meng X, Fang S, Zhang Z, et al. Preventive effect of chrysin on experimental autoimmune uveitis triggered by injection of human IRBP peptide 1–20 in mice. *Cell Mol Immunol*. 2017;14:702-711.
52. Mani R, Natesan V. Chrysin: sources, beneficial pharmacological activities, and molecular mechanism of action. *Phytochemistry*. 2018;145:187-196.
53. Lirdprapamongkol K, Sakurai H, Abdelhamed S, et al. A flavonoid chrysin suppresses hypoxic survival and metastatic growth of mouse breast cancer cells. *Oncol Rep*. 2013;30:2357-2364.
54. Han Jeong G, Cho JH, Jo C, et al. Gamma irradiation-assisted degradation of rosmarinic acid and evaluation of structures and anti-adipogenic properties. *Food Chem*. 2018;258:181-188.
55. Byun EB, Song HY, Mushtaq S, et al. Gamma-irradiated luteolin inhibits 3-isobutyl-1-methylxanthine-induced melanogenesis through the regulation of CREB/MITF, PI3K/Akt, and ERK pathways in B16BL6 melanoma cells. *J Med Food*. 2017;20:812-819.
56. Song HY, Kim HM, Mushtaq S, et al. Gamma-irradiated chrysin improves anticancer activity in HT-29 colon cancer cells through mitochondria-related pathway. *J Med Food*. 2019;22:713-721.
57. Farah M, Parhar K, Moussavi M, Eivemark S, Salh B. 5,6-Dichloro-ribifuranosylbenzimidazole- and apigenin-induced sensitization of colon cancer cells to TNF-alpha-mediated apoptosis. *Am J Physiol Gastrointest Liver Physiol*. 2003;285:G919-G928.
58. Brentnall M, Rodriguez-Menocal L, De Guevara RL, Cepero E, Boise LH. Caspase-9, caspase-3 and caspase-7 have distinct roles during intrinsic apoptosis. *BMC Cell Biol*. 2013;14:32.
59. Vélez C, Zayas B, Kumar A. Biological activity of N-hydroxyethyl-4-aza-2,3-didehydropodophyllotoxin derivatives upon colorectal adenocarcinoma cells. *Open J Med Chem*. 2014;4:1-11.
60. Krezel I. New derivatives of imidazole as potential anticancer agents. *Farmaco*. 1998;53:342-345.
61. Gao S, Siddiqui N, Etim I, Du T, Zhang Y, Liang D. Developing nutritional component chrysin as a therapeutic agent: bioavailability and pharmacokinetics consideration, and ADME mechanisms. *Biomed Pharmacother*. 2021;142:112080.